Honorable Mention Poster Award

Computerized mass detection in whole breast ultrasound images: Reduction of false positives using bilateral subtraction technique

Yuji Ikedo[a], Daisuke Fukuoka[b], Takeshi Hara[a], Hiroshi Fujita[a],
Etsuo Takada[c], Tokiko Endo[d], and Takako Morita[e]

[a]Department of Intelligent Image Information, Division of Regeneration and Advanced Medical Sciences, Graduate School of Medicine, Gifu University, 1-1 Yanagido, Gifu 501-1194, JAPAN;
[b]Technology Education, Faculty of Education, Gifu University, 1-1 Yanagido, Gifu 501-1193, JAPAN;
[c]Division of Medical Ultrasonics, Center of Optical Medicine, Dokkyo Medical University, 880 Kitakobayashi, Mibu, Tochigi 321-0293, JAPAN;
[d]Department of Radiology, National Hospital Organization Nagoya Medical Center, 4-1-1 Sannomaru, Naka-ku, Naogya, Aichi 460-0001, JAPAN;
[e]Department of Mammary Gland, Chunichi Hospital, 3-6-38 Marunouchi, Naka-ku, Nagoya, Aichi 460-0002, JAPAN

ABSTRACT

The comparison of left and right mammograms is a common technique used by radiologists for the detection and diagnosis of masses. In mammography, computer-aided detection (CAD) schemes using bilateral subtraction technique have been reported. However, in breast ultrasonography, there are no reports on CAD schemes using comparison of left and right breasts. In this study, we propose a scheme of false positive reduction based on bilateral subtraction technique in whole breast ultrasound images. Mass candidate regions are detected by using the information of edge directions. Bilateral breast images are registered with reference to the nipple positions and skin lines. A false positive region is detected based on a comparison of the average gray values of a mass candidate region and a region with the same position and same size as the candidate region in the contralateral breast. In evaluating the effectiveness of the false positive reduction method, three normal and three abnormal bilateral pairs of whole breast images were employed. These abnormal breasts included six masses larger than 5 mm in diameter. The sensitivity was 83% (5/6) with 13.8 (165/12) false positives per breast before applying the proposed reduction method. By applying the method, false positives were reduced to 4.5 (54/12) per breast without removing a true positive region. This preliminary study indicates that the bilateral subtraction technique is effective for improving the performance of a CAD scheme in whole breast ultrasound images.

Keywords: whole breast ultrasound image, computer-aided detection, bilateral subtraction

1. INTRODUCTION

Breast cancer has had the highest incident rate among all women's cancer since 1996 in Japan. Therefore, the detection and treatment of breast masses at an early stage of breast masses are important tasks for radiologists and surgeons. Currently, mammography and ultrasonography are used as reliable methods for early detection of masses in breast cancer screening. Screening using mammography has been established for women over 40 years of age with the recommendation of the government in Japan. However, it has been reported that screening using mammography together with ultrasonography is effective in the detection of breast cancer.[1–3] It response to that finding, the Japanese government decided to investigate the effectiveness of the combination screening

corresponding author email: ikedo@fjt.info.gifu-u.ac.jp

Medical Imaging 2007: Computer-Aided Diagnosis, edited by Maryellen L. Giger, Nico Karssemeijer,
Proc. of SPIE Vol. 6514, 65141T, (2007) · 1605-7422/07/$18 · doi: 10.1117/12.709225

for a five years interval between 2007 and 2011. In other words, the importance of ultrasonography in screening is gained.

Some ultrasound (US) scanners for breast cancer screening have been developed. ALOKA Co., Ltd., Japan has developed a whole breast US scanner ASU-1004. This scanner is a water path system and scans the whole breast in three overlapping runs. U-Systems, Inc. has developed automated breast US system SomoVu. This system sweeps the breast with wide-aperture linear transducer.

US images are difficult for inexperienced radiologists to interpret because the quality of US images is poorer than that of mammograms. In addition, fatigue from interpreting of a large volume of US images is another cause of oversights of masses. Therefore, computer-aided detection (CAD) schemes in assisting radiologists in detecting breast masses and providing "second opinion" have been studied by several research groups. Giger et al. have reported an automatic lesion detection technique using a radial gradient index filtering.[4–6] They have also investigated breast mass classification using a Bayesian neural network and computer-extracted lesion features.[4,5,7] Chang et al. have proposed a method that finds suspicious frames among whole breast US images using watershed segmentation.[8] They have also reported a fully automatic screening system for detection of tumor regions.[9] This system detect regions by using thresholding measure based on gray-level slicing. Fukuoka et al. have developed a CAD scheme based on active contour and balloon models in 2-D and 3-D spaces.[10] We have also reported a method for the detection of masses in whole breast US screening images.[11–13] Although a number of computerized methods for reduction of false positives were used in these reports, there are no reports on schemes using comparison of left and right breast US images. Normal left and right breasts are roughly anatomical symmetrical, radiologists use this knowledge in interpreting mammograms. In mammography, CAD schemes using bilateral subtraction technique have been reported.[14,15] In this study, we propose a scheme of false positive reduction based on bilateral subtraction technique in whole breast US images. The proposed scheme is used to improve the performance of our CAD system.[11–13] Moreover, we developed automated registration scheme to use bilateral subtraction technique.

2. MATERIALS

2.1. Data acquisition

We employed whole breast US images which were obtained by Prosound-II SSD-5500 with whole breast scanner ASU-1004 developed by ALOKA Co., Ltd., Japan. Overview of the ASU-1004 is shown in Fig. 1. This scanner has a 6cm linear transducer probe with frequency range of 6-10 MHz, and the probe moves mechanically in the water. A special membrane for US is stretched on the water and subject set her breast in a prone posture on the membrane. The probe scans an area of 16 × 16 cm^2 automatically in three overlapping runs with an overlapping area is 1 cm in width. The depth interval between two consecutive views is 0.125-2 mm.

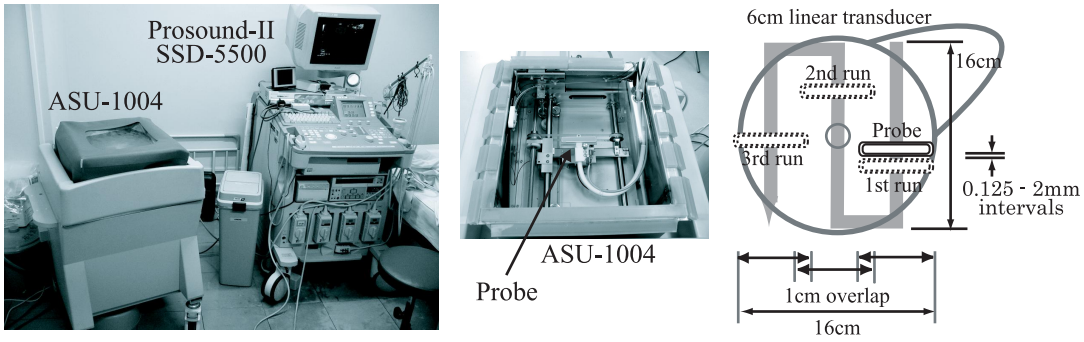

Figure 1. The whole breast ultrasound scanner ASU-1004. A breast is automatically scanned in three overlapping runs and the scanning area is 16 × 16 cm^2

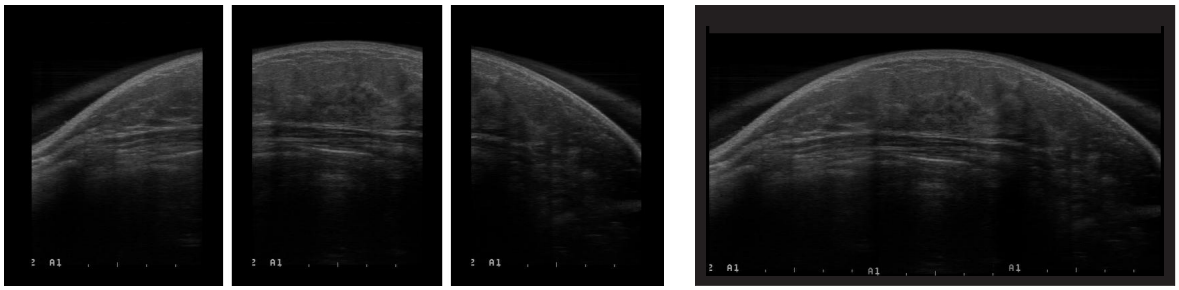

(a) (b)

Figure 2. Generation of a slice view of a whole breast. (a) The original three separate images. (b) A whole breast slice view generated by integrating the images in (a).

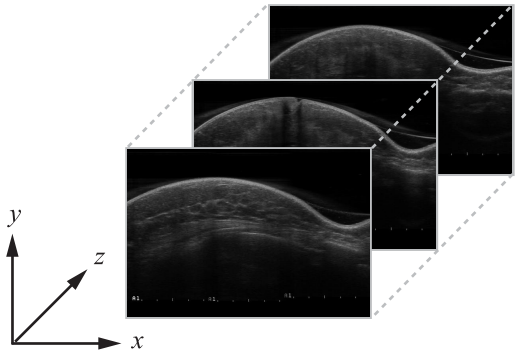

Figure 3. Definition of coordinate axis

A view is generated by integrating three separate images[13] as shown in Fig. 2. A whole breast image consists of a number of slice views as shown in Fig. 3. The coordinate system used in this manuscript is also indicated in Fig. 3.

2.2. Database

In this study, we employed whole breast images which consist of 160 - 171 slice views per breast. The distance of each slice view was 1 mm, and slice width and height was 550 - 678 pixels and 418 - 422 pixels with 256 gray-levels. Our database consisted of three normal and three abnormal bilateral pairs of whole breast cases. These abnormal breasts included six masses larger than 5 mm in diameter with one malignant mass, one fibroadenoma and four cysts. All cases were diagnosed by an experienced radiologist.

3. METHODS

In this section, first we will describe our method for masses detection. Secondly, we will introduce our proposed bilateral subtraction technique for the reduction of false positives.

3.1. Detection and segmentation of mass candidates

Mass candidates detection was previously reported.[11] A modified approach was used in this study and is described in the following.

US images are always noisy and the brightness of these images varies with the cause of different gain settings on US device. The median filter and hyteresis smoothing algorithm are applied to reduce noise and gray scale transformation is employed to normalize brightness.

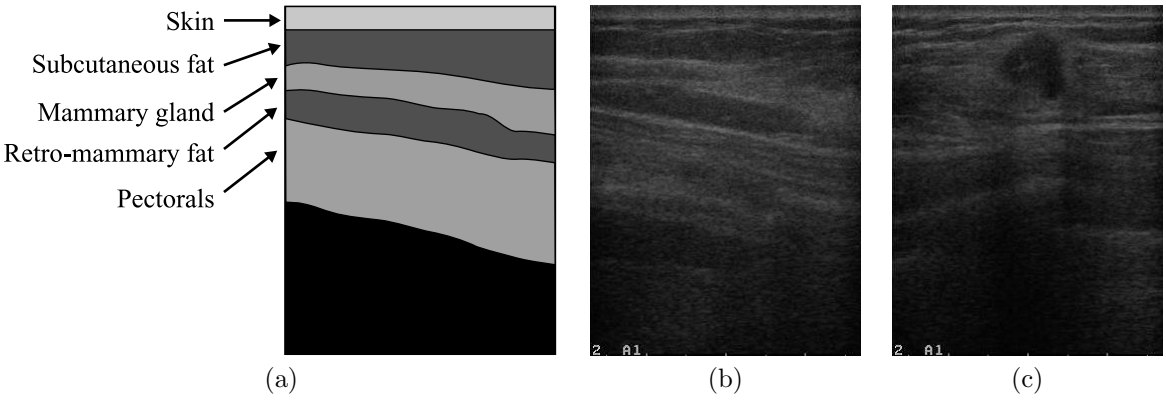

Figure 4. (a) A schematic drawing of tissue layers in breast US images. (b)A normal breast ultrasound image consisting of mainly near-horizontal edges. (c) An abnormal image with a mass showing near-horizontal and near-vertical edges.

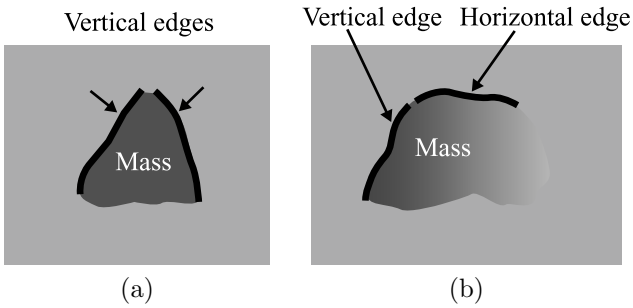

Figure 5. The combination of two edges to identify the mass candidates. (a) Two near-vertical edges. (b) A near-vertical edge and a near-horizontal edge.

The breast volumes are segmented from the background by using gray level value thresholding with a threshold level of 40 followed by a largest component selection. Connected to the image boundary and having a value of 0 are identified as the background. The breast volume is defined as the complement of the background.

Mass candidates are identified using edge directions in each breast region. A normal breast US image consist of five main kinds of tissue, skin, subcutaneous fat, mammary gland, retro-mammary fat, and pectorals, as shown in a schematic drawing in Fig. 4(a). While a normal image shown in Fig. 4(b) consists of mainly near-horizontal edges, an abnormal image shown in Fig. 4(c) includes not only near-horizontal edges but also near-vertical edges around the border of a mass. Therefore, these near-vertical edges are used as a cue to identify mass candidates and a location with two pair edges as shown in Fig. 5 is determined as a mass candidates. In order to detect edges, we adopted the Canny edge detector[16] which has a higher detection rate for the desired edges and a lower false detection rate for features that mimic the edges.

Mass candidates are segmented from the parenchymal background using the watershed algorithm.[17,18] The algorithm is one of the seed-based region growing techniques using gradient magnitude for thresholding. The largest output among the segmented regions is extracted as a mass candidate region. An example image of segmentation result is shown in Fig. 6.

For initial false positives reduction, four image features were used, i.e., average density features (ADF), difference density feature (DDF), density gradient feature (DGF), and position feature (PF). The ADF is an average density of the lowest 10% of cumulative histogram in a mass candidate region. The DDF is the difference in average densities between a core region and a periphery region in the candidate region. The DGF is a measure

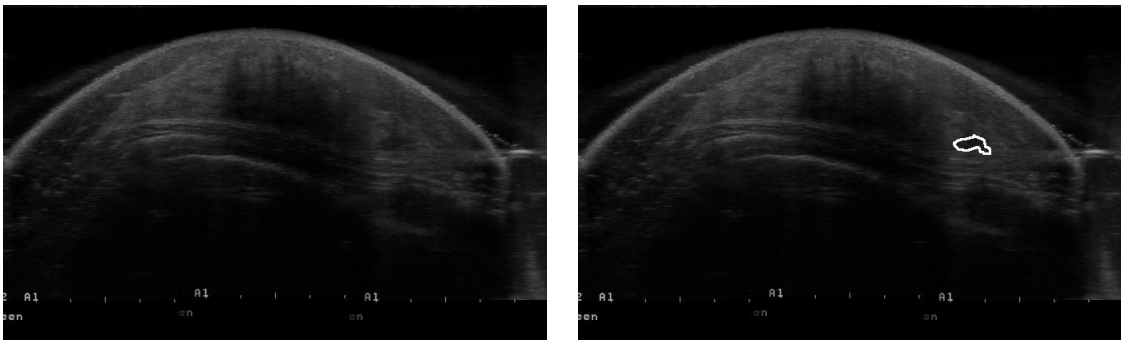

(a) (b)

Figure 6. Mass candidate segmentation. (a) Original image. (b) Computer result image with a contour line of detected mass which is a malignant mass.

of convergence of density gradient vector in a margin region on the candidate region. The PF is the vertical distance between the center of gravity (x_g, y_g) in the candidate region and the extreme bottom of the breast region (x_g, y_b). A rule-based technique based on these four features was used for initial false positives reduction.

3.2. Reduction of false positives based on bilateral subtraction technique

3.2.1. Comparing bilateral breasts

Normal left and right breasts on same subject are architectural symmetry. The symmetrical feature is employed by radiologists as a useful tool in interpreting mammograms. Even if there is such a region like a mass, the region is classified normal tissue if same position in the other breast image has similar feature region. We employed this feature to reduce false positives in US images. The overall computerized bilateral subtraction technique involves: (1) image feature extraction; (2) registration of bilateral breasts; and (3) reduction of false positives. Three-dimesional breast images are used in all of the above procedures.

3.2.2. Image feature extraction

In order to align the left and right breast images, landmarks are needed to establish the correspondence between the bilateral breast images. Skin line in each of slice view and nipple positions are extracted as landmarks for such correspondence.

Fig. 7 shows average gray value of tissue-classified in a whole breast slice view after preprocessing. Each tissue region was segmented manually. Skin region is depicted as the highest gray value of all tissues in whole breast images. Initial skin regions are segmented from other tissue and the background by using gray level value thresholding with a threshold level of 200. The segmented region with largest volume is determined as a skin region of all other segmented regions. However, skin region is not segmented accurately, because part of skin regions could be depicted lower gray value than the threshold level due to the nipple and artifact. Therefore, skin region is approximated as a 2-variable polynominal of degree 2 by least squares method and the polynominal is defined as the skin line $S(x, y_S, z)$ which is used as the breast border. The y-coordinate, y_S, the skin line on a view is given by

$$y_S = \sum_{k=1}^{3} \sum_{m=1}^{k} a_{(k-1)k/2+m} x^{k-m} z^{m-1}, \tag{1}$$

where a_i is coefficient value of the polynominal.

To locate the nipple position, profile of the local gray value along the skin line is used. Fig. 8 shows a breast slice view containing the nipple. Acoustic shadow posterior to the nipple is evidence and will decrease the average gray level value in the vicinity of the nipple. Details of the procedure are described in the following.

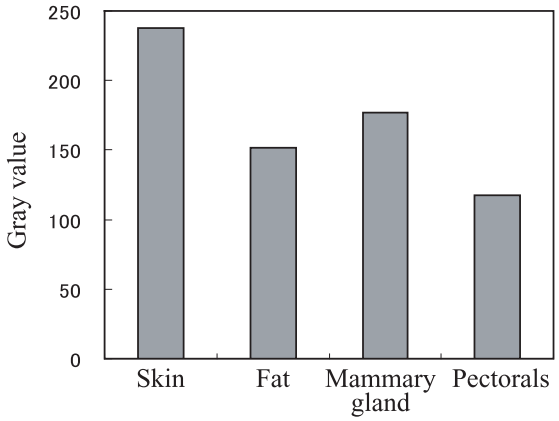

Figure 7. Average gray value of tissue-classified in a whole breast slice view after preprocessing.

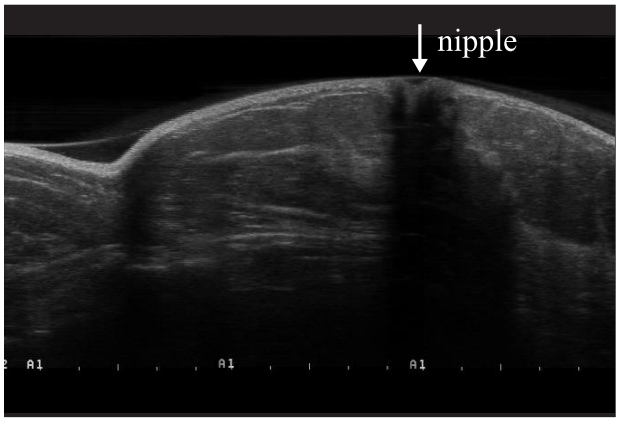

Figure 8. Example of acoustic shadow caused by nipple.

First a nipple slice z_N is determined using average gray value in a volume of interest (VOI). A nipple position is located near the point with maximum value of y-axis in a breast region. The pixel of the point with maximize value of y_S in each slice is defined as $(x', y'_S, k) \in S(x, y_S, z), k = 1, 2, \ldots, n$. A profile is calculated along the (x', y'_S, k) in each slice k, where average gray value at (x', y'_S, k) is obtained by averaging the gray values within the VOI, 40 by 10 by 13 mm in size. Fig. 9 shows an example of a profile obtained with this method. The slice with the lowest average gray value in the VOI is determined as a nipple slice z_N.

Secondly, nipple position (x_N, y_S, z_N) is determined using average gray value in a VOI. A profile is calculated along the $(i, y_S, z_N), i = 1, 2, \ldots, m$ in nipple slice z_N, where average gray value at (i, y_S, z_N) is obtained by averaging the gray values within the VOI, 13 by 10 by 13 mm in size. Fig. 10 shows an example of a profile obtained with this method. The position with the lowest average gray value in the VOI is determined as a nipple postion (x_N, y_S, z_N).

3.2.3. Registration of bilateral breasts

A right whole breast is defined as a reference breast and a left whole breast is defined as a target breast. The left breast is transformed to align with the right breast. The target breast is shifted to align the nipple position

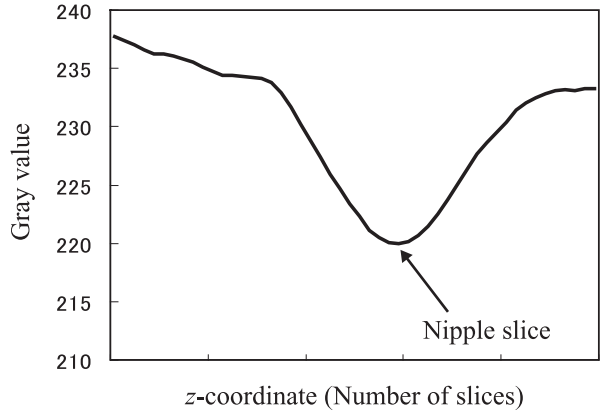

Figure 9. An average profile calculated along the (x', y'_S, k) in each slice view, where average gray value at (x', y'_S, k) is obtained by averaging the gray values within a volume of interest. The arrow indicates the nipple slice number.

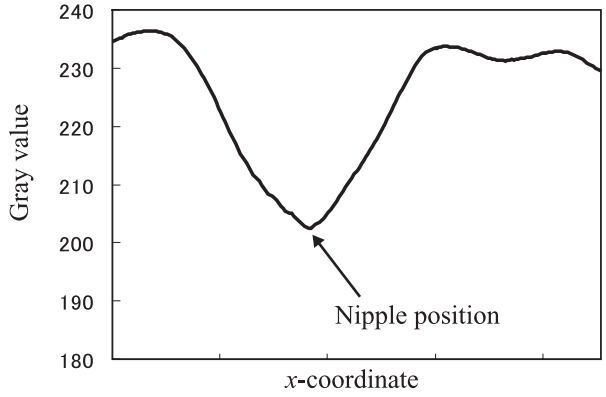

Figure 10. An average profile calculated along the (i, y_S, z_N) in nipple slice, where average gray value at (i, y_S, z_N) is obtained by averaging the gray values within a volume of interest. The arrow indicates the nipple position.

to the reference breast nipple position. The translation vector $\boldsymbol{T}$ is given by

$$\boldsymbol{T} = \boldsymbol{N}_R - \boldsymbol{N}_L, \tag{2}$$

where $\boldsymbol{N}_R$ and $\boldsymbol{N}_L$ are the right and left breast nipple positions. Moreover, the shifted target breast $B_L(i, j, k)$ is transformed to $B'_L(i, j + d, k)$ to align the skin line with the skin line of reference breast. The translational interval d is given by

$$d = y_{SR} - y_{SL}, \tag{3}$$

where y_{SR} and y_{SL} are the right and shifted left breast skin lines.

Example slices after implementation of the registration is shown in Fig. 11.

3.2.4. Reduction of false positives

An average gray value of a mass candidate region detected by the above mentioned method is denoted as I_m, and the value of a region with the same position and same size as the mass candidate region in the contralateral breast is denoted as I_c. If the gray value difference D given by $D = I_c - I_m$ is lower than the threshold value,

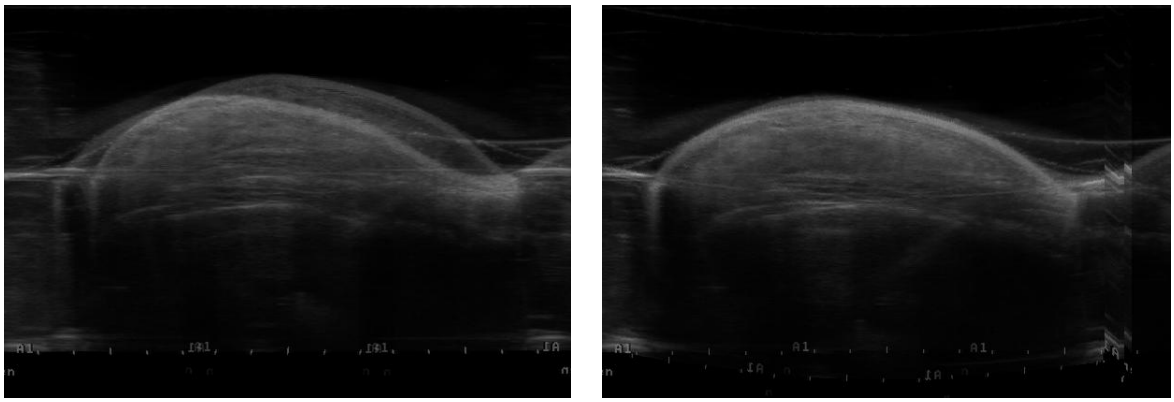

(a) (b)

Figure 11. Left and right breast fusion image. (a) Fusion image before registration (b) Fusion image after registration.

the mass candidate region is eliminated as a false positive. The threshold value was 30 which was selected empirically.

4. RESULTS

The false positive reduction scheme based on bilateral subtraction technique described here was evaluated using our database mentioned in Section 2. Table 1 shows the performance of our detection method without the subtraction technique and with the technique. The true positive (TP) rate of mass was 83% (5/6) both with and without the technique. In contrast, the number of false positives (FPs) per breast before applying the technique and after applying the technique were 13.8 (165/12) and 4.5 (54/12) per breast, respectively.

Example images of accurately reduced regions as a false positive are shown in Fig. 12. Left breast image in Fig. 12 is registered and row 1 shows original images with a rectangle of region of interest (ROI). Row 2 shows closeup images of the ROI. Solid contours described in row 2 images indicate false positive regions. These regions are correctly eliminated by our proposed false positives reduction method using bilateral subtraction technique.

5. DISCUSSION

It was found that a scheme of false positive reduction based on bilateral subtraction technique in whole breast US image can effectively reduce false positives because 67.3 % false positives were eliminated without removing a true positive region. However, many false positives in the regions posterior to nipples were not detected. This was because acoustic shadows formed in these regions varied due to slight differences in the nipple sizes and shapes. Consequently, shadow regions in bilateral breast images are not all the same and many false positives were not detected.

Table 1. Performance of proposed mass detection scheme without the subtraction technique and with the technique.

	TP	FP/breast
without	83% (5/6)	13.8 (165/12)
with	83% (5/6)	4.5 (54/12)

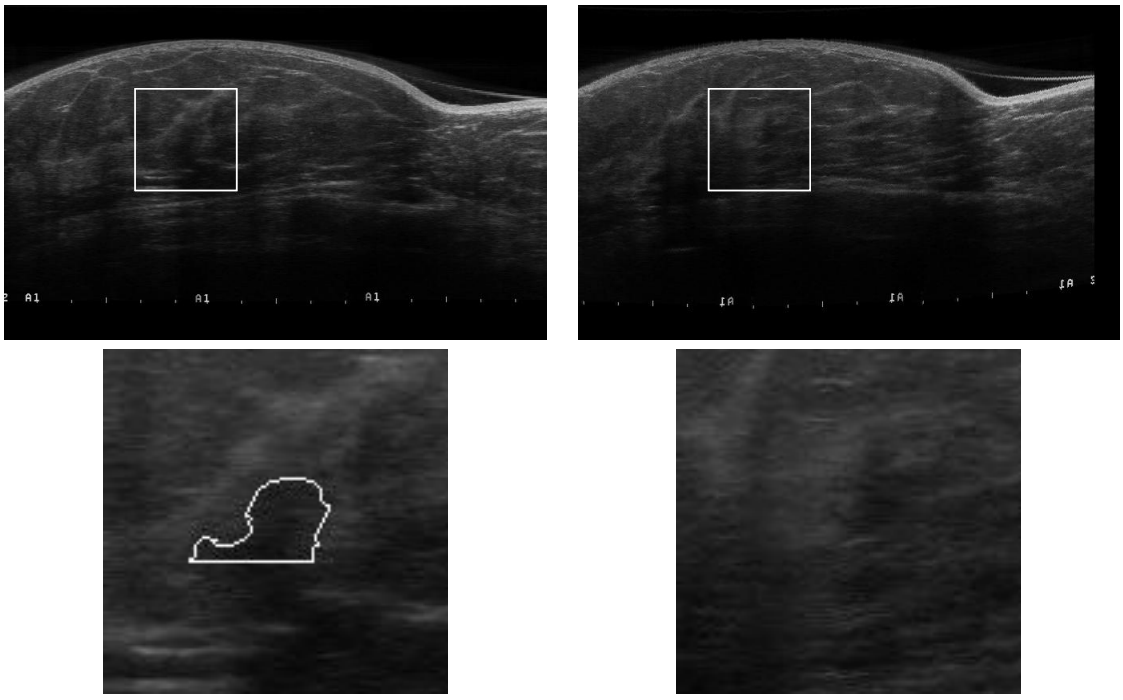

Figure 12. Examples of false positives reduction. Row 1: An original right breast image and a registrated left breast breast image with rectangular of region of interests (ROI) as marked; row 2: Closeup images of the ROI. Solid contour described in row 2 image is a false positive region. This region is accurately eliminated as a false positive region by our proposed false positive reduction method using bilateral subtraction technique.

6. CONCLUSION

We proposed a bilateral subtraction technique to reduce false positives in mass candidate regions detected by our detection scheme for whole breast US images. By using the method, the performance of our CAD system was improved. It was found that the bilateral subtraction technique could reduce false positives effectively. In the future, it is necessary to develop a method to reduce false positive regions in posterior to the nipple and to confirm experimentally the reliablity and accuracy of the bilateral subtraction technique by employing a larger database.

ACKNOWLEDGMENTS

This work is supported in part by a grant for the Knowledge Cluster Gifu-Ogaki, the Grant-in-Aid for Young Scientists (B), 167907 and the Research on Priority Area from Ministry of Education, Culture, Sports, Science and Technology, JAPAN. This work was supported in part by cancer research funds from Ministry of Health and Welfare, Japan. The authors are grateful to ALOKA CO., LTD., Japan and TAK CO., LTD., Japan for their assistance in this study. The authors would like to thank Dr. G. Lee for improving the manuscript, and other members of Fujita Laboratory in Graduate School of Medicine, Gifu University, Japan for their helpful comments and discussions.

REFERENCES

1. T. M. Kolb, J. Lichy, and J. H. Newhouse, "Comparison of the performance of screening mammography, physical examination, and breast us and evaluation of factors that influence them: an analysis of 27,825 patient evaluations," *Radiology* **225**, pp. 165–175, 2002.

2. K. Flobbe, P. J. Nelemans, A. G. H. Kessels, G. L. Beets, M. F. von Meyenfeldt, and J. M. A. van Engelshoven, "The role of ultrasonography as an adjunct to mammography in the detection of breast cancer: a systematic review," *European Journal of Cancer* **38**, pp. 1044–1050, 2002.
3. D. B. Kopans, "Breast-cancer screening with ultrasonography," *Lancet* **354**, pp. 2096–2097, 1999.
4. K. Drukker, M. L. Giger, K. Horsch, M. A. Kupinski, and C. J. Vyborny, "Computerized lesion detection on breast ultrasound," *Med. Phys.* **29**, pp. 1438–1446, 2002.
5. K. Drukker, M. L. Giger, , C. J. Vyborny, and E. B. Mendelson, "Computerized detection and classification of cancer on breast ultrasound," *Acad. Radiol.* **11**, pp. 526–535, 2004.
6. M. A. Kupinski and M. L. Giger, "Automated seeded lesion segmentation on digital mammograms," *IEEE Trans. Med. Imaging* **17**, pp. 510–517, 1998.
7. K. Horsch, M. L. Giger, L. A. Venta, and C. J. Vyborny, "Computerized diagnosis of breast lesions on ultrasound," *Med. Phys.* **29**, pp. 157–164, 2002.
8. R. F. Chang, K. C. Chang-Chien, H. J. Chen, D. R. Chen, E. Takada, and W. K. Moon, "Whole breast computer-aided screening using free-hand ultrasound," in *Computer Assisted Radiology and Surgery*, H. U. Lemke, K. Inamrua, K. Doi, M. W. Vannier, and A. G. Farman, eds., *Proc. of CARS* **2005**, pp. 1075–1080, 2005.
9. R. F. Chang, C. J. Chen, E. Takada, C. M. Kuo, and D. R. Chen, "Image stitching and computer-aided diagnosis for whole breast ultrasound image," in *International Journal of Computer Assisted Radiology and Surgery*, H. U. Lemke, K. Inamrua, K. Doi, M. W. Vannier, and A. G. Farman, eds., *Proc. of the 20th International Congress and Exhibition* **1**, pp. 340–343, 2006.
10. D. Fukuoka, T. Hara, H. Fujita, T. Endo, and Y. Kato, "Automated detection and classification of masses on breast ultrasonograms and its 3D imaging technique," in *5th International Workshop on Digital Mammography*, M. J. Yaffe, ed., *Proc. of IWDM 2000*, pp. 182–188, 2001.
11. Y. Ikedo, D. Fukuoka, T. Hara, H. Fujita, E. Takada, T. Endo, and T. Morita, "Computer-aided detection system of breast masses on ultrasound images," in *SPIE Medical Imaging 2006: Image Processing*, J. M. Reinhardt and J. P. W. Pluim, eds., *Proc. of SPIE* **6144**, pp. 61445L1–61445L8, 2006.
12. Y. Ikedo, D. Fukuoka, T. Hara, H. Fujita, E. Takada, T. Endo, and T. Morita, "Fully automatic detection system for breast masses on ultrasound images," in *International Journal of Computer Assisted Radiology and Surgery*, H. U. Lemke, K. Inamrua, K. Doi, M. W. Vannier, and A. G. Farman, eds., *Proc. of the 20th International Congress and Exhibition* **1**, p. 519, 2006.
13. D. Fukuoka, Y. Ikedo, T. Hara, H. Fujita, E. Takada, T. Endo, and T. Morita, "Development of breast ultrasound cad system for screening," in *Digital Mammography*, S. M. Astley, M. Brady, C. Rose, and R. Zwiggelaar, eds., *8th International Workshop, IWDM 2006, Manchester, UK, June 2006, Proceedings*, pp. 392–398, 2006.
14. F. F. Yin, M. L. Giger, K. Doi, C. J. Vyborny, and R. A. Schmidt, "Computerized detection of masses in digital mammograms: Automated alignment of breast images and its effect on bilateral-subtraction technique," *Med. Phys.* **21**, pp. 445–452, 1994.
15. F. F. Yin, M. L. Giger, K. Doi, C. E. Metz, C. J. Vyborny, and R. A. Schmidt, "Computerized detection of masses in digital mammograms: Analysis of bilateral subtraction images," *Med. Phys.* **18**, pp. 955–963, 1991.
16. J. F. Canny, "A computational approach to edge detection," *IEEE Trans. Pattern Anal. Mach. Intell.* **8**, pp. 679–698, 1986.
17. Y. L. Huang and D. R. Chen, "Watershed segmentation for breast tumor in 2-d sonography," *Ultrasound in Medicine & Biology* **30**, pp. 625–632, 2004.
18. L. Vincent and P. Soille, "Watersheds in digital spaces: An efficient algorithm based on immersion simulations," *IEEE Trans. Pattern Anal. Mach. Intell.* **13**, pp. 583–598, 1991.